Lake Tahoe Clarity Analysis and Modeling: Empirical Dynamic Modeling

John M. Melack[1] and Ethan R. Deyle[2]

1. Bren School of Environmental Science and Management, University of California, Santa Barbara, CA 93106

2. Department of Biology, Boston University, Boston, MA 02215

Summary

Water clarity and related conditions in Lake Tahoe result from complex interactions among the physics, chemistry and ecology of the lake and its surroundings. These factors vary by season and have changed over years due to management actions and natural variability. The interconnections and interdependencies among these factors makes forecasts quite challenging. An approach that extracts information directly from data with few assumptions to forecast expected conditions, called empirical dynamic modeling, has been successfully applied to other complex systems, such as fisheries and financial markets. Forecasting success depends on the inherent properties and representativeness of the available data. Empirical dynamic modeling (EDM) uses time-series data to construct a representation of a system's dynamics, and is fundamentally different from traditional simulation models and statistical methods. We evaluated the ability of EDM to analyze and possibly forecast clarity and related conditions based on data spanning several decades for Lake Tahoe.

A subset of measurements from Lake Tahoe with the longest, most complete records were selected for investigation: Secchi depths, chlorophyll a and nitrate concentrations, lake temperatures, stream discharge, precipitation, air temperature, and climate indices. Initial analyses demonstrated the forecast skill using EDM for Secchi depth, nitrate, and chlorophyll-a were moderate to high. Further analyses with EDM techniques revealed a strong effect of precipitation on Secchi depth and indicated a nonlinear dependence on conditions in the lake. Greater forecast skill using EDM in comparison to linear statistics for water quality variables (Secchi depth, chlorophyll-a, and nitrate) using climatic drivers (stream discharge, El Nino index, and precipitation) provides solid evidence of complex coupling among factors. Though a causal effect of El Nino state on Secchi depth was found, its predictive skill was less than proximate drivers, such as stream discharge and precipitation. The results indicate the importance of direct, nonlinear forcing of clarity by stream discharge.

Introduction

Empirical dynamic modeling is an approach for analyzing ecosystem dynamics derived from theoretical work on the dynamical behavior of nonlinear, coupled systems (Sugihara and May 1990; Deyle and Sugihara 2011; Sugihara et al. 2012). Nonlinearity means that the behavior of a system (how its parts interact with each other) will change as the overall system changes. This means that particular relations may unexpectedly change, or even switch from positive to negative, as a result of system changes. Such systems must be studied synergistically – they cannot be studied one factor at a time. For example, the factors and their interactions that determine clarity in lakes represent a nonlinear, dynamic system in that important variables and their relations to each other change as conditions in the lake vary.

EDM uses time-series data with minimal assumptions to construct a representation of the system's dynamics that accommodates nonlinear behavior. It is a fundamental departure from traditional algebraic or simulation models and statistical methods that are based on fixed relations, and is gaining traction in a variety of fields including ecology and for ecological forecasting (e.g., Hsieh et al. 2005; Perretti et al. 2013; Deyle et al. 2013; Ye et al. 2015; McGowan et. al. 2017, Ushio et. al. 2018; Munch et al. 2018; Chang et al. 2020, Cenci et al. 2020, Nova et al. 2021). An example of EDM's utility is provided by an analysis of larval supply, a critical aspect of recruitment and a challenge in fisheries management (Dixon et al. 1999). By clever selection of surrogates for deterministic (lunar state) and stochastic (wind stress) factors, the nonlinear dependencies of larval supply were revealed. A recent application to Lake Geneva (France/Switzerland) illustrates how EDM can improve understanding of trends in eutrophication associated with management of nutrient inputs and climate changes (Deyle et al. 2022).

The EDM approach has the advantage of capturing relations among variables through time, when individual, mechanistic interactions are difficult to model (Munch et al. 2020). Furthermore, a common problem with parametric simulation models is called equifinality, i.e., different model structures and parameter sets produce similar results. This is partially addressed in EDM by applying a causality test (convergent cross mapping; Sugihara et al. 2012) to narrow the number of possible variables to those that are observed to have exerted measurable causal influence. As noted by Mooji et al. (2010), a complementary approach is to combine empirical (inductive) elements derived from data and parameterized (deductive) elements derived from first principles. An example of this hybrid approach with EDM applied to Lake Geneva is described in Deyle et al. (2022).

We provide theoretical and conceptual background and a brief description of the steps used by EDM in Appendix 1 and include the data with metadata in Appendix 2.

EDM application to Lake Tahoe

The specific goal of the application of EDM to Lake Tahoe is to evaluate its ability to forecast clarity and related conditions based on time-series data. More general goals are to investigate the viability of empirical dynamic modeling for supporting water-quality management of Lake Tahoe, including forecasting of future management scenarios and clarifying mechanistic hypotheses about the drivers of water clarity changes. The analysis consisted of three phases: 1) data evaluation and processing. 2) single-variable forecast analysis, and 3) causal analysis of core variables.

EDM depends on the time-series of data to represent the system's dynamics. Hence, we selected measurements with the longest, uninterrupted records. Though measurements with

short records, such as inputs of fine suspended particles, or with incomplete sampling, such as zooplankton and phytoplankton abundances, are relevant to variations in clarity, they are not readily amenable to EDM analyses.

Data used

Among the datasets available, a subset was selected for investigation with EDM based on the length and frequency of collection and relevance to clarity:

Secchi depths (UC Davis): LTP – 1967 to 2020 (every ca.13 days)

Chlorophyll a (UC Davis): LTP – 1983 to 2020; 0, 2, 5, 10, 15, 20, 30, 40, 50, 60, 75, 90, 105 m (depth averaged for upper 30 m and lower depths)

Nitrate (UC Davis): LTP – 1968 to 2020 (every ca.13 days until 2007, and then monthly; 0, 2, 5, 10,15, 20, 30, 40, 50 m (depth averaged)

Lake temperatures (UC Davis): LTP -1967 to 2020 every ca. 13 days)

Stream discharge with USGS codes (https://nwis.waterdata.usgs.gov/nwis/uv/):

Upper Truckee River at South Lake Tahoe, CA - UT1 10336610 from 1980

Blackwood Creek near Tahoe City, CA - BC1 10336660 from 1974

Ward Creek at Hwy 89 near Tahoe Pines, CA - WC8 10336676 from 1972

Precipitation and air temperature (National Weather Service via Truckee River Operating Agreement; https://www.troa.net/tis/):

Daily precipitation and average of maximum and minimum temperatures at Tahoe City from 1937; TROA – site 150017 (Lake Tahoe) variables 1616 and 8.

https://www.troa.net/tis/?interval=day&type=1&cat=1&sid=150017&did11=1616&did13=8&format=tab&sdate=01-JAN-1960&edate=01-Apr-2022

Climate Indices: (https://psl.noaa.gov/data/climateindices/)

El Nino 3.4 index and SOI are monthly indicators of the state of El Nino Southern Oscillations based on sea surface temperature averages and east-west sea surface pressure differences, respectively.

Initial data processing

Given the different sources and kinds of measurements, we accepted most data as provided. Since time-series analysis prefers regular sampling intervals, and the data vary in frequency of collection, we generated two-monthly and, for comparison, three-monthly averages. As an example, Figure 2 illustrates Secchi depth measurements for a two-year period with both the two-month and three-month averages.

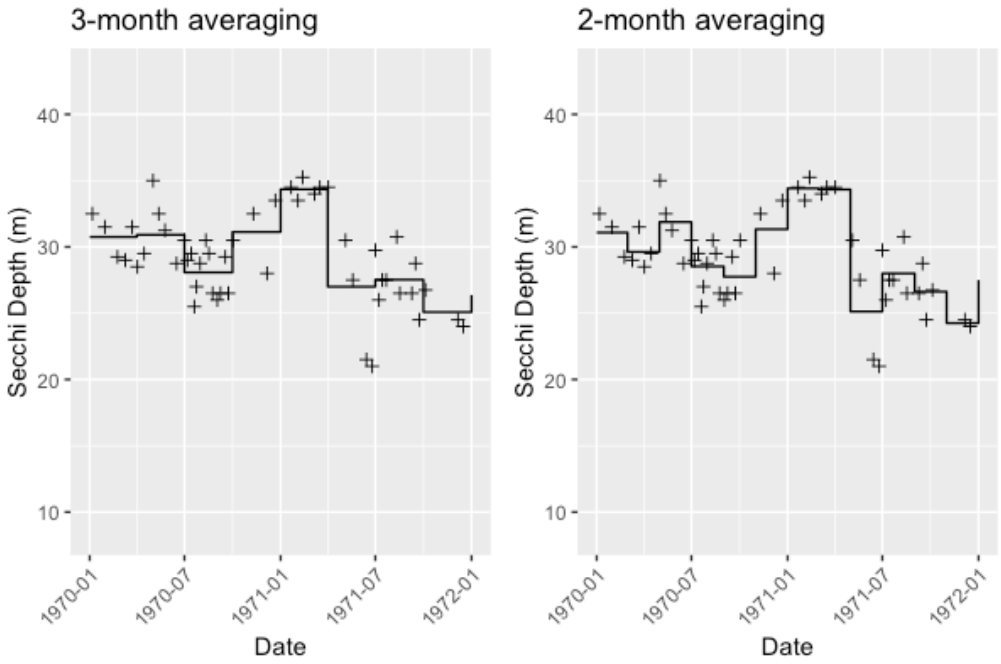

Figure 2. Secchi depths (m) at LTP from 1970 to 1972 with two-month and three-month binned averages shown as a continuous black lines. + indicate individual measurements.

We defined two depths to compute a limnologically-informed depth average for chlorophyll a (Chl-a) and nitrate: the upper 25 m, i.e. the region within most Secchi depths and the deeper euphotic zone (to about 90 m). We weighted the averages based on the distance between successive depth measurements to reduce the influence of occasional missing data at individual depths. We also processed the data with no weighting to check that our weighting scheme did not produce artefacts.

Figure 3 illustrates the time-series data used in the EDM analyses. Data files with metadata are available as appendices in two forms: "Tahoe_limnological data.csv" contains the variables Secchi depth, chlorophyll-a, and nitrate for the historical period (01-1967 to 09-2020). "Tahoe_limnological data_and_drivers.csv" contains the analyzed drivers for the period with consistent overlap (11-1983 to 09-2020).

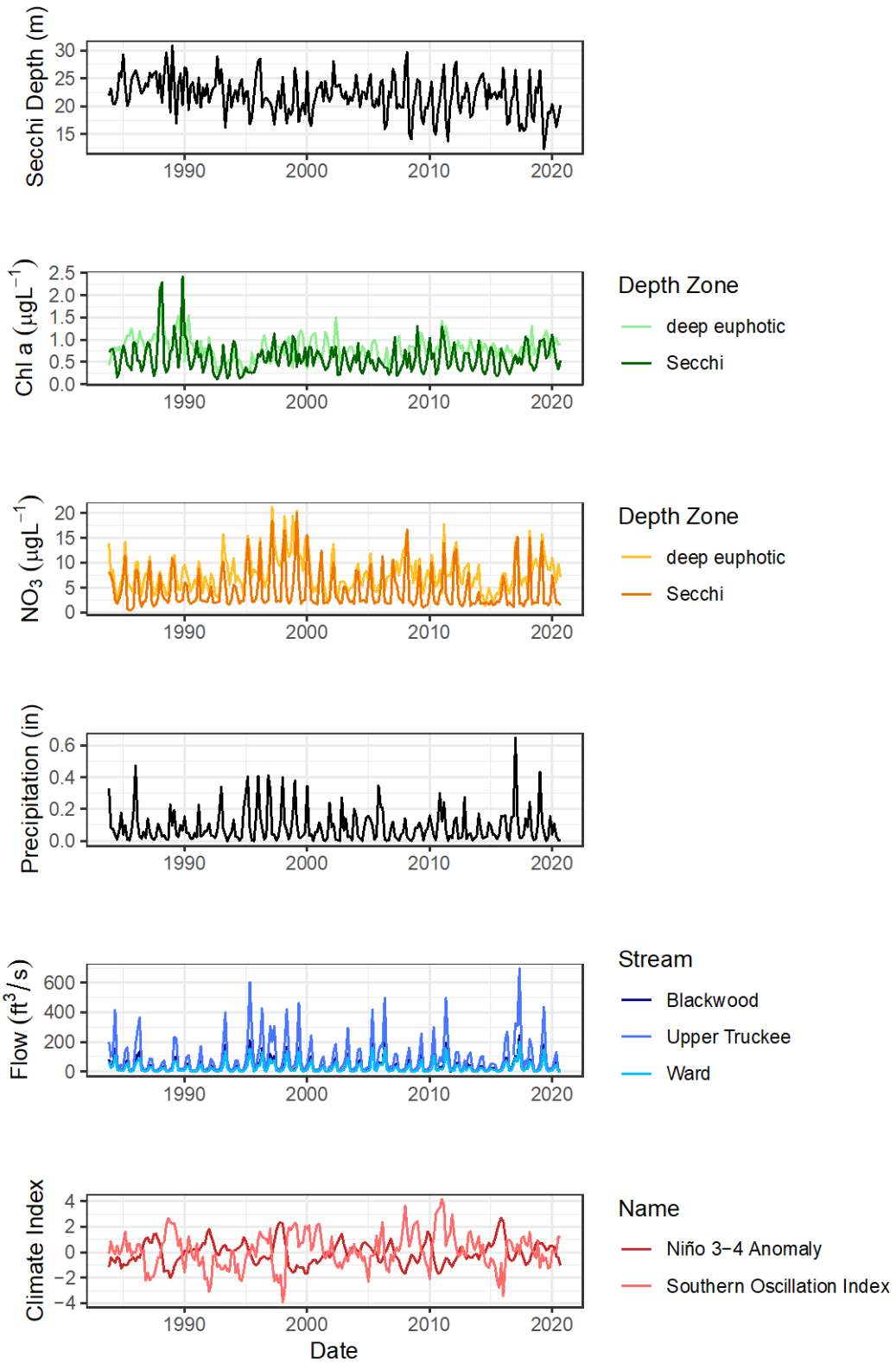

Figure 3. Time series of variables after processing in 2-month intervals. Biogeochemical variables Chl a and NO_3 were depth averaged over two intervals: upper 25 m (Secchi) and ~30 to 90 m (deeper euphotic zone).

Single-variable forecast analyses

Single-variable forecast analyses can help distinguish hypotheses about underlying mechanisms and serve as a foundation for subsequent causal and quasi-mechanistic modeling by providing 1) guidance on parameters, such as time averaging, and 2) guidance on assumptions in further analysis, i.e., the existence of low-dimensional attractor dynamics that help explain changes in time-series variables. EDM methods, including CCM, simplex and S-mapping, are described in Appendix 1.

The fundamental output of univariate EDM analysis is forecast skill, i.e. the correspondence between the historical observed values and the model predicted values. Here, we use Pearson's correlation (ρ) between observed and predicted values to quantify how much of the historical variance is recovered in the predictions. Error measures such as mean absolute error and root-mean squared error can also be used; note that forecast error is reciprocal of forecast skill. For Pearson's correlation, $\rho = 0$ indicates a lack of forecast skill and $\rho = 1$ indicates perfect forecast skill. Significant forecast skill suggests that there are low-dimensional nonlinear dynamics underlying variables; in this case, related to the water quality of Lake Tahoe.

Among Secchi depth, NO_3, and Chl-a, forecast skills ranged from 0.4 – 0.8 with simplex projection and S-map. By standard Gaussian statistics, these values are all statistically significant, i.e. that chances of measuring these levels of forecast skill for purely random Gaussian data are very nearly zero. However, dynamics of natural systems rarely follow simple rules represented by Gaussian statistical models and have secular changes over years, seasonal variations, experience extreme events, and have other behaviors. These factors can all create degrees of non-random forecast skill that is not evidence of underlying dynamics. Hence, to assess the statistical power and significance, we used null surrogate methods. Surrogates generate random data that preserve basic properties of the system, such as seasonal variations or long-term trends, but randomize other variation. We used three such 'null hypotheses' for the interpretation of our results:

> Null hypothesis 1: Prediction skill is due to *random* chance. If the prediction skill is due to random chance, then randomly shuffling the sequence of the observations would generate similar forecast skills for the surrogate time series as our analysis of the real data.
>
> Null hypothesis 2: Prediction skill is due to temporal *persistence*, i.e. serial autocorrelation in the time series. If the prediction skill measured in the historical time series is due solely to autocorrelation of the observations, then a random realization of an autoregression process with the same temporal persistence would generate similar forecast skills for the surrogate time series as our analysis of the real data.
>
> Null hypothesis 3: Prediction skill is due to *seasonal* variations. If prediction skill is due to the inherent seasonality of the system, then randomized deviations from the long-term seasonal average would generate similar forecast skills for the surrogate time series as our analysis of the real data.

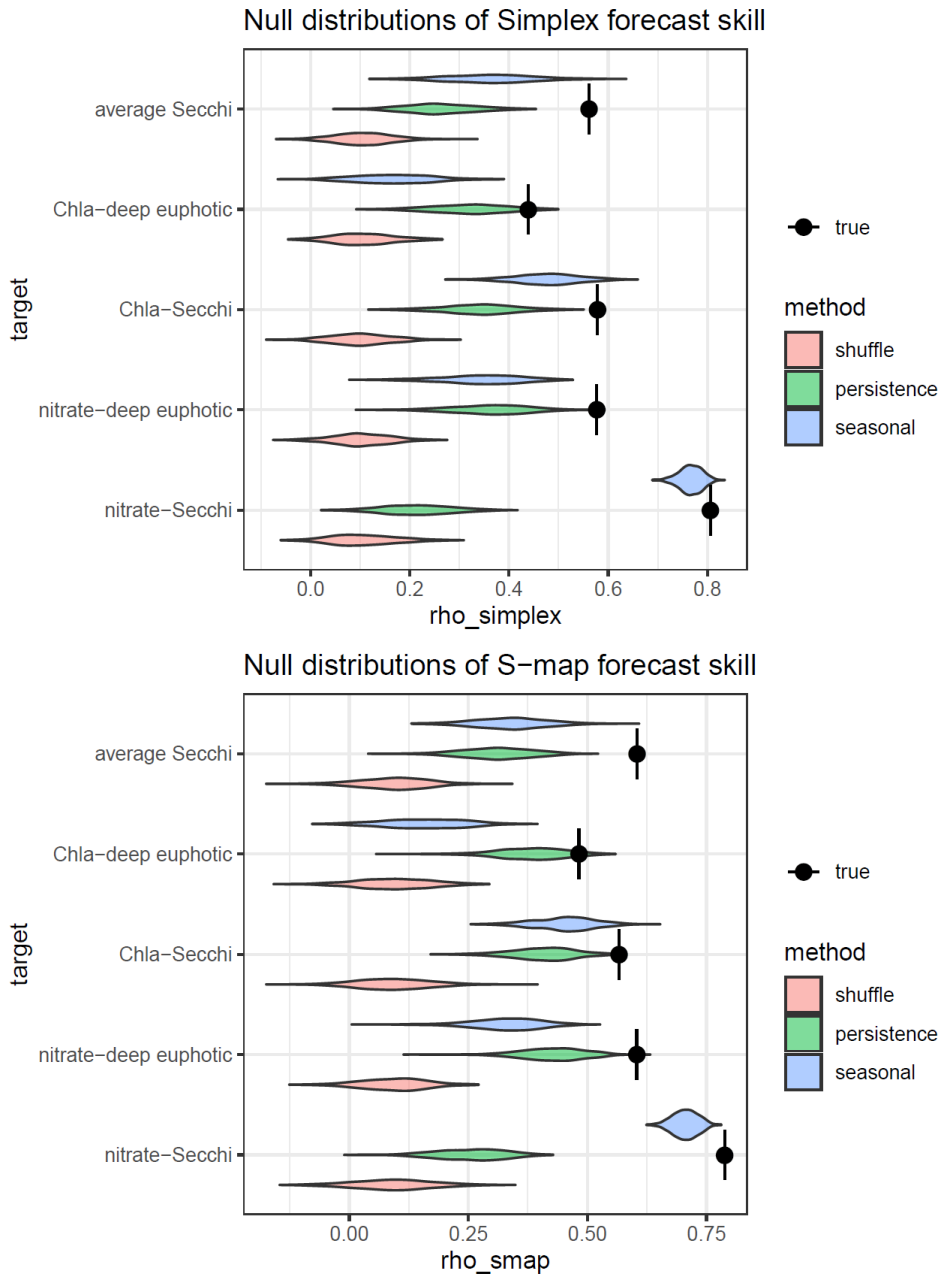

Figure 4. Summary of univariate analyses and null distributions indicating predictability of limnological variables (and suitability to EDM analysis). The true level of the EDM forecast skill (using either simplex projection or S-map) is shown as a black dot with a vertical bar to indicate exact level. This true level is then compared to the distribution of forecast skill for surrogate (null) time series generated by three different methods, each corresponding to a different null hypothesis. In both simplex and S-map forecasts, the true level (skill measured for the true time series) are usually higher than the levels measured on surrogates indicating that we can reject the null hypothesis in those cases. We do find that there is substantial long-term forecast skill partly due to the underlying seasonality of the system.

In all cases, predictive skills are greater than expected for random data with the same distribution of values (i.e., 'shuffle' surrogates) (Figure 4). The autocorrelation and seasonal variation surrogates do suggest some predictive skill, though the EDM results have greater predictive skill, in general, than that of these two surrogates. Overall, there is clear evidence of low-dimensional behavior, i.e. predictable change over time based on a few variables and interactions. This behavior reflects underlying processes that determine the lake's ecology and climate variables that are predictable, but not effects of climate drivers that themselves are not predictable, i.e., 'stochastic drivers'.

EDM causal analyses

To examine the key drivers of clarity and water quality, lagged statistical relationships were computed and compared to nonlinear causal metrics.

Lagged statistical correlations: The 2-month averaged discharges in the Upper Truckee River and in Ward and Blackwood creeks are highly correlated with each other at 0-lag. However, the Upper Truckee River has missing measurements (~1460 days), while Ward Creek has few missing data and was used to represent variations in discharge. Physical drivers acting on the lake probably do not have immediate influence; therefore, time-lag relations were examined. For example, the 'cross-correlation function' between Ward Creek discharge and precipitation at Tahoe City indicates that Ward Creek discharge is most strongly associated with a 4-month lag (2 time-steps of 2-month averaged data; Figure 5)

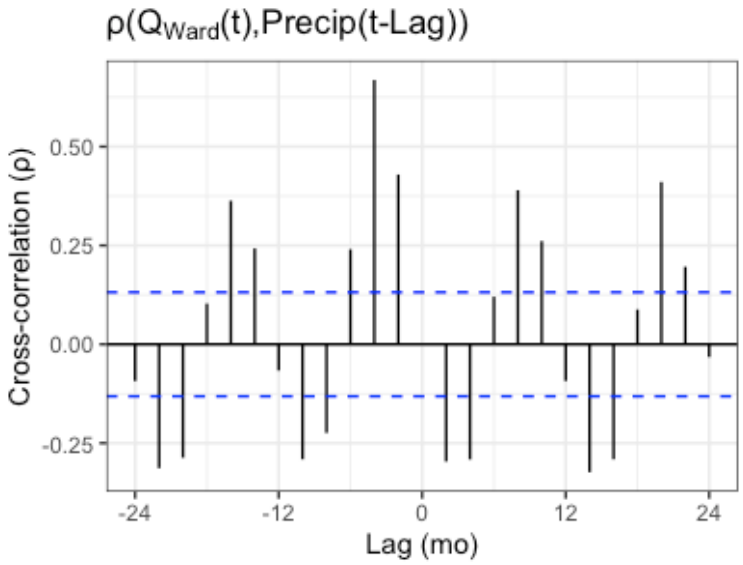

Figure 5. Time-lagged correlation analysis of streamflow and precipitation. The Pearson correlation coefficient between streamflow at Ward Creek, $Q_{Ward}(t)$, and time-lagged precipitation, Precip(t-Lag), is shown as a function of the Lag. The 2-month increments in time-lag value occur because these time series have been processed in 2-month increments. The blue dotted lines represent 95% confidence intervals based on standard Gaussian statistics. The maximum association between these variables is observed between Q_{Ward} and Precip 4-months previous.

Nonlinear coupling relationships: Evidence of coupling among variable was next examined using the time-series forecasting framework of convergent cross-mapping (CCM), that tests if the sequence of changes in one variable predicts those in another variable. Figure 6 is an example of CCM analysis of coupling between precipitation and Secchi depth. Unlike correlation analysis, the cross-map skill is a directional measurement, i.e. ρ_{CCM}(secchi –> precip) ≠ ρ_{CCM}(precip –> secchi). That being said, in the presence of strong, unidirectional forcing (so-called 'environmental synchrony'), there may be measurable cross-map skill in the reverse direction when there is no bidirectional coupling.

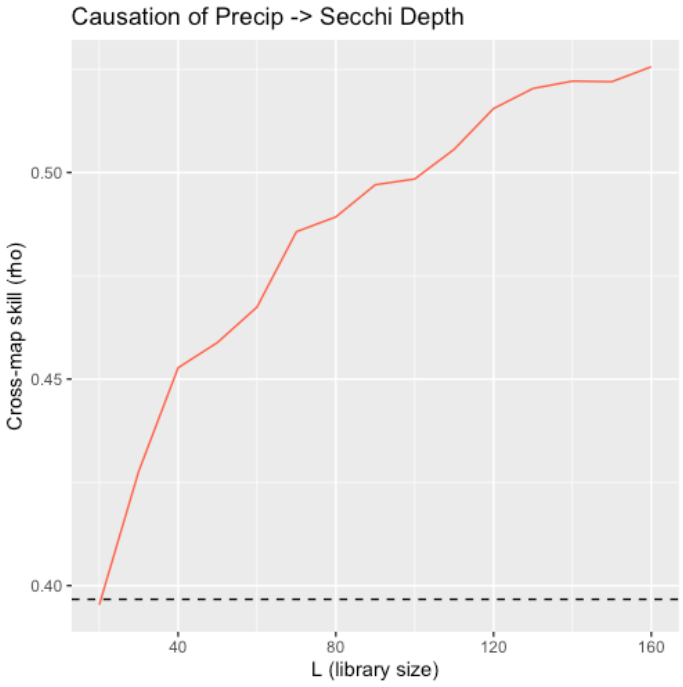

Figure 6. Example of convergent cross-mapping for the dynamic relationship between Secchi depth and precipitation. To assess evidence of a causal effect between variables X and Y, CCM uses the accuracy of cross-predicting values of *X* with Simplex projection from the reconstructed attractor of *Y*. As a larger library of points are used for the prediction, forecast skill improves, indicating the prediction skill is not merely due to a static linear correlation between the variables. The dotted black line shows as reference the maximum magnitude of the lagged linear correlation between the variables. The presence of a significant correlation suggests a strong effect of the causal variable, precipitation, on the response, Secchi depth. Moreover, the increase in cross-map skill above this level with increasing library size indicates a nonlinear state-dependence in this relationship beyond simple passive tracking.

Since both the cross-map skill and linear correlations are quantified by Pearson's correlation coefficient for explained variance, they can, at least superficially, be directly compared. Lagged correlation analysis for the same coupling (Secchi depth and precipitation) is shown in Figure 7. While there is a lagged linear relationship between precipitation and Secchi

depth, the dynamic causal method explains greater variance (Figure 6). Hence, there is evidence of a complex coupling between weather and clarity.

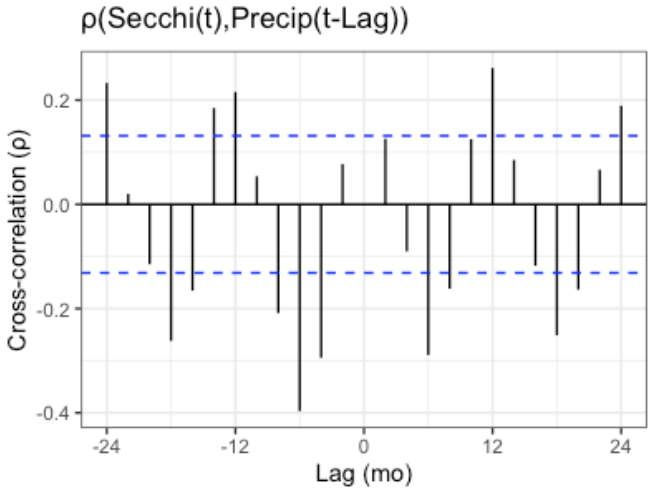

Figure 7. Time-lagged correlation analysis of Secchi depth and precipitation. The Pearson correlation coefficient between Secchi depth and time-lagged precipitation is shown as a function of the time lag. The 2-month increments in time-lag value are because these time series have been processed in 2-month increments. The blue dotted lines represent 95% confidence intervals based on standard Gaussian statistics. Both positive and negative cross-correlations are of interest.

Comparison between CCM skill (ρ_{CCM}) and the lagged linear correlation (ρ_{corr}) for key water quality variables (Secchi depth, chl-a, and nitrate) and the climatic drivers (stream discharge, El Nino index, and precipitation) are provided in Table 1. CCM skill greater than lagged linear correlations ($\rho_{CCM} > \rho_{corr}$) is evidence of complex coupling, i.e. state-dependent interaction. In particular, this comparison helps assess net effects and evidence of the importance of individual pathways from large-scale climate variables to the lake clarity. The El Nino index has the signature of causal effect on Secchi depth (ρ_{CCM}), but its predictive skills are smaller than more proximate drivers, such as stream discharge and precipitation. Overall, the results indicate the importance of direct, nonlinear forcing by stream discharge.

A key need is forecasting and understanding impacts of environmental factors, such as climatic conditions (e.g., ENSO events) and related variables, such as precipitation and stream discharge, on clarity and water quality. One goal of causal analysis is to assess the net effect and evidence for the relative importance of individual pathways. That being said, a direct comparison of ρ_{CCM} across variables requires additional analysis, such as the use of seasonal surrogates to account for underlying predictability of driving variables. For example, depth-averaged lake temperature and stream flow both have a strong seasonal periodicity. Multivariate prediction, pursued as the final step of analysis, further examines these relations.

Table 1. Comparison of cross-map skill to static correlation between climate drivers and limnological variables. Maximum predictive skill of nonlinear convergent cross-mapping (ρ_{CCM}) and predictive skill of the optimal lagged linear correlation (ρ_{corr}) are listed. Significantly higher skill in the nonlinear test, i.e. $\rho_{CCM} > \rho_{corr}$, is evidence of complex coupling between variables.

variable	**driver**	ρ_{ccm} ρ_{corr}
Chla-deep euphotic	Niño 3.4	0.28 0.19
Chla-deep euphotic	precip	0.46 0.31
Chla-deep euphotic	Q_{Ward}	**0.57** 0.30
Chla-deep euphotic	T-deep euphotic	0.60 0.34
Chla-deep euphotic	T-Secchi	**0.75** 0.33
Chla-Secchi	Niño 3.4	0.17 0.13
Chla-Secchi	precip	0.56 0.39
Chla-Secchi	Q_{Ward}	**0.67** 0.40
Chla-Secchi	T-deep euphotic	0.73 0.50
Chla-Secchi	T-Secchi	**0.92** 0.57
NO_3-deep euphotic	Niño 3.4	0.37 0.26
NO_3-deep euphotic	precip	0.61 0.44
NO_3-deep euphotic	Q_{Ward}	**0.73** 0.56
NO_3-deep euphotic	T-deep euphotic	0.82 0.55
NO_3-deep euphotic	T-Secchi	**0.92** 0.48
NO_3-Secchi	Niño 3.4	0.22 0.14
NO_3-Secchi	precip	0.65 0.62
NO_3-Secchi	Q_{Ward}	**0.79** 0.74
NO_3-Secchi	T-deep euphotic	0.86 0.66
NO_3-Secchi	T-Secchi	**0.96** 0.72
average Secchi	Niño 3.4	0.45 0.18
average Secchi	precip	0.56 0.40
average Secchi	Q_{Ward}	**0.68** 0.41
average Secchi	T-deep euphotic	0.62 0.39
average Secchi	T-Secchi	**0.76** 0.43

Based on CCM skills, we can identify hypotheses about drivers. The Niño 3.4 index does show evidence of a causal effect on Secchi depth, though the prediction skills are smaller than the proximate physical drivers of stream discharge and precipitation. The highest CCM skill for all variables is shown to be lake temperature, specifically averaged over the Secchi zone (< 30 m). In all cases, the CCM skill is higher than expected based on simple time-lagged corrleations, which indicates that ecological variables in Lake Tahoe are sensitive to temperature, and that

responses depend on the state of the lake and wider system. Linear correlations between precipitation and average Secchi depth are similar to those between the stream discharge and average Secchi depths. However, the CCM skill is distinctly larger for the stream discharge than precipitation. The same pattern applies to chlorophyll-a and NO_3. The maximum lagged correlations of stream discharge and precipitation on these variables are similar, but the CCM skill is notably higher.

EDM multivariate prediction

A further question is if understanding causal drivers, i.e. expanding the dimensions of variability, can lead to improved forecasting. Though a full multivariate forecasting analysis is beyond the scope of the current analysis, univariate EDM predictions may be improved by incorporating causal drivers as done by Deyle et al. (2013). As noted above, cross-map analysis indicates that stream discharge is a more proximate driver of Secchi depth than lake temperature. Thus, EDM forecast skill was examined by adding one or both of these variables to standard univariate lagged coordinate embedding. Given the seasonal dynamics of these variables, it is important to also include a direct indicator of season, e.g. a sine wave that tracks the Earth's orbit. This allows improved forecast skill to be distinguished from shared seasonal forcing.

The S-map analysis shows that incorporating streamflow as a driver of Secchi depth has value beyond just representing the common seasonality of all the interconnected lake variables. Incorporating stream discharge (Q) leads to a clear improvement of forecast skill, while lake temperature (T) does not (Figure 8). This forecast skill is on par with the improved skill by incorporating the seasonal cycle (season). However, the greatest forecast skill is achieved by incorporating both stream flow and the seasonal cycle.

An important insight from this analysis is key to further time-series approaches to examination of Lake Tahoe's water quality. While suggestive, the initial analysis (Figure 4) did not show unequivocal evidence for underlying endogenous limnological dynamics driving water clarity, while Figure 8 does. The seasonal cycle is explicitly included as an embedding variable, and while significant predictability is evident with one coordinate dimension, predictability substantially increases by adding lags (E) of the target variable, Secchi depth.

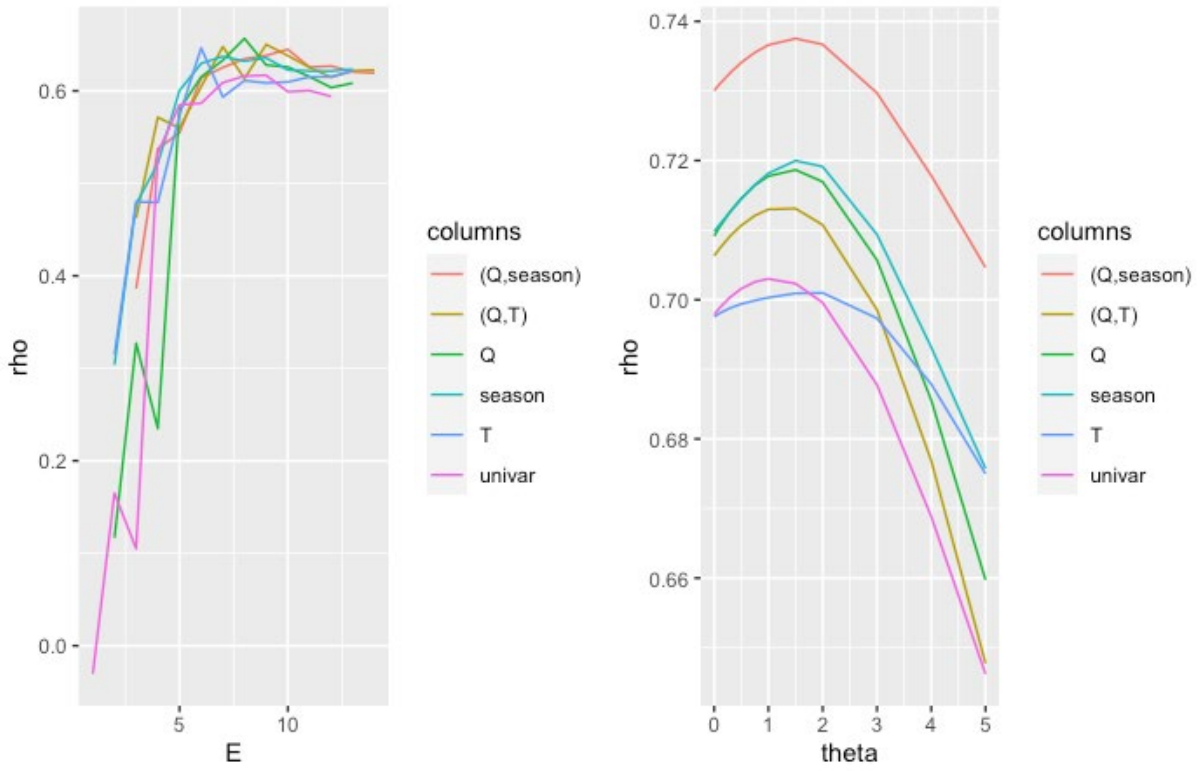

Figure 8. Forecast skill improvement with climate drivers. The univariate EDM forecast skill analyzed and plotted in Figure 4 (labeled "Univar") is compared to forecast skill when one or more of the identified driving variables are incorporated as dimensions of variability. (Left) For each line, the starting point on the left incorporates only the climate drivers. In all cases this captures a part of the variability. Adding additional dimensions (increasing E) increases predictability and indicates that there are additional drivers of variation beyond those identified here. Notably this applies not only to streamflow (*Q*) and lake temperature (*T*) but also to the underlying seasonal cycle itself. (Right) Using these mixed multivariate embeddings, S-map forecasting was applied to assess how much interdependence between drivers affects forecast skill. In all cases, a nonlinearly tuned S-map (theta > 0) performs better than the linear S-map (theta = 0).

Future directions

As further work, a full multivariate forecasting analysis done and additional variables could be examined. Deyle et al (2022) provides an example of a full multivariate analysis with EDM of the biogeochemical variables associated with water quality in Lake Geneva. They were able to identify a set of variables that predicted deep-water dissolved oxygen concentrations, and to estimate interaction rates between variables as they changed through season and time. Several of variables relevant to current understanding of Tahoe clarity are available only since 2008 (e.g., fine suspended particles), or have substantial data gaps (e.g., phytoplankton counts, zooplankton surveys. To use such data would require exploration of techniques using surrogates to generate longer datasets and testing forecast skill with available data.

Acknowledgements

We thank the California Natural Resources Agency for funding (Work Order #106-UCSB; TRPA Contract #19C00008), Robert Larsen (TSAC) for administrative support, Shohei Watanabe (UC Davis) for providing data files, and George Sugihara (UC San Diego) and Geoff Schladow (UC Davis) for advice and comments.

References (including Appendix 1 citations)

Cenci, S., Medeiros, L.P., Sugihara, G., and Saavedra, S. 2020. Assessing the predictability of nonlinear dynamics under smooth parameter changes. J. Royal Society Interface. 17, 20190627.

Chang, C.-W., Ye, H., Miki, T., Deyle, E.R., et al. 2020. Long-term warming destabilizes aquatic ecosystems through weakening biodiversity-mediated causal networks. Global Change Biol. 26: 6413–6423.

Deyle, E. and Sugihara, G. 2011. Generalized theorems for nonlinear state space reconstruction. PLoS ONE 6: e18295. doi:10.1371/journal.pone.0018295.

Deyle, E.R., Fogarty, M.J., Hsieh, C.H., Kaufman, L., et al. 2013. Predicting climate effects on Pacific sardine. Proc. Natl. Acad. Sci. USA. 110: 6430–6435.

Deyle, E.R., May, R.M., Munch, S.B., and Sugihara, G. 2016. Tracking and forecasting ecosystem interactions in real time. Proc. Royal Soc. B. 283, 20152258.

Deyle, E., Bouffard, D., Frossard, V., Schwefel, R., Melack, J., and Sugihara, G. 2022. A hybrid empirical and parametric approach for managing ecosystem complexity: Water quality in Lake Geneva under nonstationary futures. Proc. Natl. Acad. Sci. USA. 119, e2102466119. doi.org/10.1073/pnas.2102466119

Dixon, P.A., Milicich, M.J., and Sugihara, G. 1999. Episodic fluctuations in larval supply. Science 283: 1528-1530.

Hsieh, C.-H., Glaser, S.M., Lucas, A.J., and Sugihara, G. 2005. Distinguishing random environmental fluctuations from ecological catastrophes for the north Pacific Ocean. Nature 435:336–340.

McGowan, J. A., Deyle, E.R., Ye, H., Carter, M.L., et al. 2017. Predicting coastal algal blooms in southern California. Ecology 98: 1419-1433.

Mooij, W.M., Trolle, D., Jeppesen, E., Arhonditsis, G., et al. 2010. Challenges and opportunities for integrating lake ecosystem modelling approaches. Aquatic Ecology 44: 633–667.

Munch, S.B., Giron-Nava, A., and Sugihara, G. 2018. Nonlinear dynamics and noise in fisheries recruitment: A global meta-analysis. Fish and Fisheries 19: 964-973.

Munch, S.B., Brias, A., Sugihara, G., and Rogers, T.L. 2020. Frequently asked questions about nonlinear dynamics and empirical dynamic modelling. ICES J. Marine Sci. 77: 1463–1479.

Nova, N., Deyle, E.R., Shocket, M.S., MacDonald, A.J., et al. 2021. Susceptible host availability modulates climate effects on dengue dynamics. Ecology Lett. 24: 415-425.

Perretti, C.T, Munch, S.B., and Sugihara, G. 2013. Model-free forecasting outperforms the correct mechanistic model for simulated and experimental data. Proc. Natl. Acad. Sci. USA. 110: 5253–5257.

Sauer, T., Yorke, J.A., and Casdagli, M. 1991. Embedology. J. Stat. Phys. 65: 579–616.

Sugihara, G. and May, R.M. 1990. Nonlinear forecasting as a way of distinguishing chaos from measurement error in time series. Nature 344: 734-741.

Sugihara, G. 1994. Nonlinear forecasting for the classification of nature time series. Philosophical Trans. Royal Society A. 348: 477–495.

Sugihara, G., May, R., Ye, H., Ysieh, C.-H., Deyle, E., Fogarty, M., and Munch, S. 2012. Detecting causality in complex ecosystems. Science 338: 496-500.

Takens, F. 1981. Detecting strange attractors in turbulence. Page 366-381. In D.A. Rand and L.S. Young (eds.). Dynamical Systems and Turbulence. Springer-Verlag, New York.

Ushio, M., Hsieh, C.H., Masuda, R., Deyle, E.R., et al. 2018. Fluctuating interaction network and time-varying stability of a natural fish community. Nature, 554: 360-363.

Ye, H., Beamish, R.J., Glaser, S.M., Grant, C.H., et al. 2015. Equation-free mechanistic ecosystem forecasting using empirical dynamic modeling. Proc. Natl. Acad. Sci. USA 112: 1569–1576.

Appendix 1

Theoretical and conceptual background

Complex systems typically experience transitions through time between different states. Each state can be represented as a vector of state variables $\underline{x}(t)$ (e.g., Secchi depth, temperature), and the set of all states that a dynamic system tends to settle to and transitions through forms a geometric construct known as an attractor manifold, ***M***. The manifold describes how ecosystem state variables relate to each other through time. If there are rules governing ecosystem changes (i.e., if ecosystem variation is not random), there is an attractor manifold to be uncovered (Deyle and Sugihara 2011). Attractor manifolds express relationships among variables and can be obtained from time- series data. Constructing attractor manifolds empirically from ecological time series is the basis of EDM. Figure 1 illustrates three core aspects. Three brief videos provide further explanation: introduction to attractors and time-series: https://www.youtube.com/watch?v=fevurdpiRYg; single time-series attractor reconstruction: https://www.youtube.com/watch?v=QQwtrWBwxQg; and attractor cross-mapping for causal inference: https://www.youtube.com/watch?v=NrFdIz-D2yM.

1) Nonlinear state dependence (panel a). If there is an attractor manifold ***M***, that is not linear, relationships between variables will depend on system state (e.g., Y_1 and Y_3 are positively correlated at some times (in some regions of the attractor) and negatively associated at other times (in other regions of the attractor)). Such state dependence is the defining hallmark of nonlinear systems and is how nonlinearity is measured in ecological time series (e.g., as accomplished by S-maps, Sugihara 1994).

2) Time series as observation functions (panel b). A time series $\{Y_i\}$ is a projection of the dynamics occurring on ***M***. More generally, Y_i are observational functions of the dynamics on ***M***. The Y_i may be fundamental coordinates or they may be any function that maps points in ***M*** to a scalar time-series variable (also known as an "observation function" on ***M***). A key point is that ecological time series can appear complex because they are projections into one dimension of dynamics occurring in higher dimensions.

3) State space reconstruction and Takens theorem (panel c). If all the variables and equations governing an ecosystem are known, we could construct the attractor manifold by direct simulation; very seldom is this the case. Alternatively, it is possible to reconstruct the manifold empirically, if we have time series for all the relevant variables. This manifold would be an empirical expression of the dynamic relationships among variables observed in the data. However, in practice we may not know what the full set of variables should be, and because of practical constraints we usually only have time series information for a subset of the variables. A key result from dynamical system theory, the Takens embedding theorem (Takens 1981) and its various extensions (Sauer et al. 1991; Deyle and Sugihara 2011) proves that in most cases one can reconstruct the dynamical attractor for a system from data of lagged samples of just one variable, such as Y_i. That is, in general interacting variables share information about each other so that any single variable contains information about the rest, and as a result, one can construct a proxy attractor (shadow manifold) for the original system that has a 1:1 correspondence (is diffeomorphic) with the original native system. Thus, state space reconstruction is a method to recover an approximation of ***M*** from time series. This is illustrated in panel c, where the shadow manifold, $\boldsymbol{M}_1$' is constructed using lags of time series $\{Y_1\}$. The reconstruction captures the essential topology and dynamics of the original system. Further refinements to this idea include multivariate reconstructions that are more mechanistic (Dixon et al. 1999; Deyle and Sugihara

2011), detecting and incorporating exogenous stochastic inputs, and exploring environmental scenarios (Deyle et al. 2013; Deyle et al. 2022).

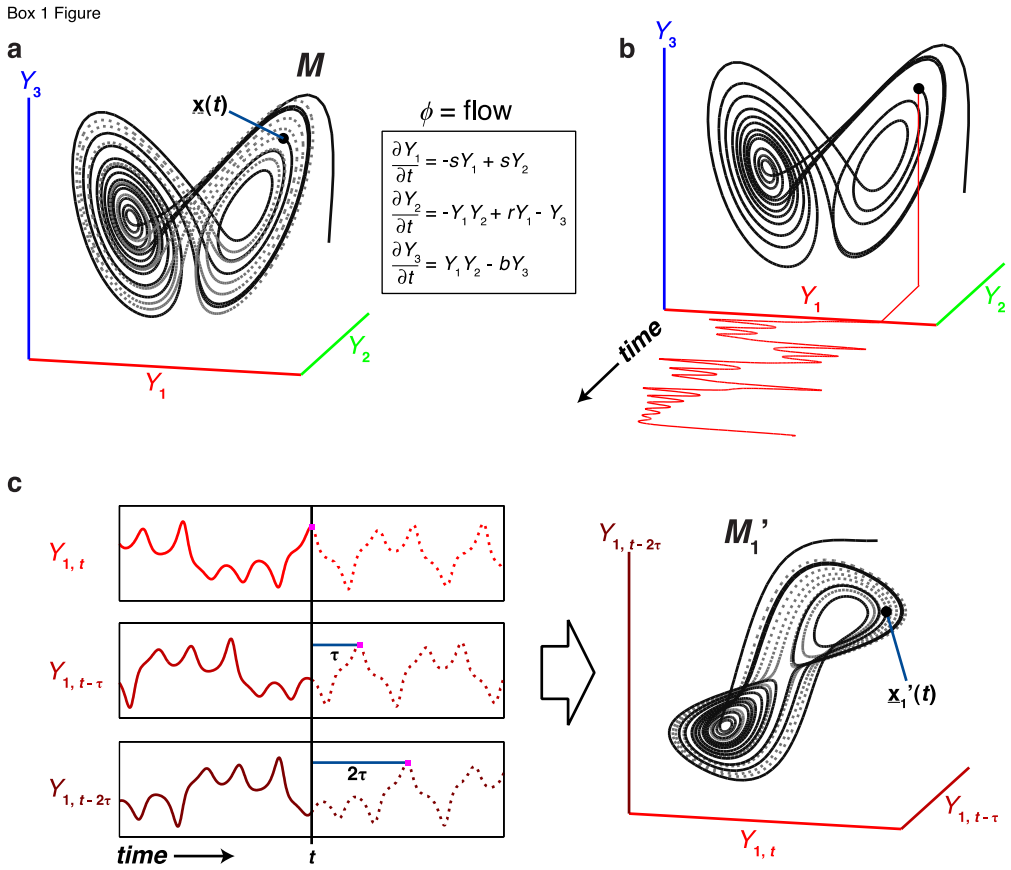

Figure 1. a) The Lorenz butterfly attractor example. The attractor manifold ***M*** is the set of states that the system progresses through. $\underline{x}(t)$ is the state of the system at time t, and the dynamics are defined by the Lorenz equations. **b)** A time series is a projection of the system states from ***M*** to a coordinate axis (Y_1 is a state variable of the system). The manifold can be constructed from the component time series**. c)** Following Takens theorem, lags of the time series $\{Y_1\}$ can act as coordinate axes to construct a shadow manifold $\boldsymbol{M}_1$'which maps 1:1 to the original manifold ***M*** (note visual similarity between $\boldsymbol{M}_1$' and ***M***). These shadow manifolds can be used for ecosystem-based prediction, identifying causal variables.

EDM methods

An initial two-step procedure is followed: 1) simplex-projection (Sugihara and May 1990) is a 0th-order 1-parameter (or at most 2-paramenters) forecasting method used to determine if the data allows prediction, and most importantly, in the process of exploring predictability it identifies the best embedding dimension (E) or number of active coordinates required to attain a given level of forecast skill; 2) this (E) is used in the S-map procedure (Sugihara 1994) to assess the nonlinearity of the time series. In both cases, model performance is evaluated either using simple cross validation, or when sufficient data are available, with the time series divided into halves so that half of the data is used to build the model and the other

blind half is used to test the predictions. This forecast protocol is a transparent rigorous standard that avoids model over-fitting or arbitrary fits to the data.

Simplex projection is a 0^{th} order nearest-neighbor forecasting algorithm that involves tracking the forward evolution of nearby points on an attractor, and as a first step in data exploration this typically involves an attractor reconstructed from lagged coordinates (Takens 1981). Thus, similar past events (nearby points on the attractor) are used to forecast the future. Thus, similarity is based on not just a single scalar value ($x_{t1} \sim x_{t2}$) or points nearby in time but on the *E*-dimensional vector of values representing a similar sequence of values through time (similar history fragments of length *E*), ($x_{t1} \sim x_{t2}$ and $x_{t1-1} \sim x_{t2-1}$ and $x_{t1-2} \sim x_{t2-2}$,… $x_{t1-(E-1)} \sim x_{t2-(E-1)}$). That is, the embedding dimension (*E*) is the amount of history required to uniquely specify a trajectory (or the number of dimensions needed to untangle trajectories of an attractor). In other words, (*E*) is the length of the historical sequence of past events needed to uniquely specify where the system is headed next.

Thus, forecasting requires transforming the scalar time series into a multidimensional vector space, called an "embedding". Given a *library set* (a set of points used to construct the model attractor) of *N* points, an *E*-dimensional embedding is generated from the time-series data using lagged coordinates so that each point in the space represents a sequence of "E" points $X(t) = \{x_t, x_{t-\tau}, x_{t-2\tau} \ldots x_{t-(E-1)\tau}\}$. Again, these vectors are generally split into library and prediction sets, $\{X_{lib}\}$ and $\{X_{pred}\}$. For each vector $X(t)$ in the prediction set, $\{X_{pred}\}$, the $E+1$ neighbors (closest points by Euclidian distance) from the library set $\{X_{lib}\}$ are identified. The forecast is based on the average of how these nearby library points (domain simplex) move forward in time, weighted by their distance. The key step for EDM is transforming a sequence of values (time series) into multidimensional vectors (embedding).

S-maps are 1^{st} order function approximation, and thus look superficially like standard linear autoregressive (AR) models. Whereas in an AR model the coefficients are computed once (applying singular value decomposition once globally) over the entire time series or set of points used to build the model (the library set X_{lib}), with nonlinear S-maps the coeffcients are computed separately for each point on the attractor. That is, in nonlinear S-maps, the coefficients depend on the location of the predictee Y_t in an *E*-dimensional embedding. Thus, new coefficients are recalculated (from the library set X_{lib}) by singular value decomposition (SVD) for each new prediction. In this calculation, the weight given to each vector in the library depends on how close that vector $X(t')$ is to the predictee $X(t)$. The extent of this weighting is determined by a nonlinear tuning parameter (or *locality* parameter), θ. When $\theta = 0$ all points are weighted equally, which produces a single global linear mapping identical to the linear AR model. Here every point on the attractor (a flat hyperplane in this case) has the same coefficents: the S-map coefficientsneed not to be computed multiple times but are computed once globally using SVD on all data in the *library* or fitting set for model. Increasing values of θ give increasingly local or nonlinear mappings where the coefficients computed by SVD differ at each point on the attractor. In the case where $\theta > 0$, vectors closest to the predictee in state-space are weighted more heavily in the SVD calculation. Such forecasts emphasize local information in the library set. If forecast performance improves for $\theta > 0$ the attractor has curvature, meaning the dynamics are not globally fixed (globally linear) but are state dependent. Dynamics that are different in different parts of the attractor are nonlinear. S-maps provide a means to quantify the nonlinearity of a time series. They also produce minimally-assumptive forecasts, that because they are 1^{st} order rather than 0^{th} order, often perfrom better than simplex.

Convergent cross mapping (CCM) is the further application of EDM to reveal the actual

dynamic relationships among variables decipherable from observational time series. CCM exploits a consequence of Takens' theorem - any one variable in a dynamic system contains information about all the other causal variables. Thus, the attractor pattern recovered from one variable can be used not just to predict future values of that one variable, but also other coupled variables that have been observed. CCM uses the forecast skill of this cross-prediction between variables to establish causation (Sugihara et. al 2012). If one variable contains dynamic information that can be used to predict the state of another this is evidence of a dynamic causal connection.

Generally, Simplex projection is used for cross-prediction. Given two aligned time series X and Y of N points, an E-dimensional embedding is generated from the time series of X using lagged coordinates so that each point in the space represents a sequence of 'E' points $X(t) = \{x_t, x_{t-\tau}, x_{t-2\tau} \ldots x_{t-(E-1)\tau}\}$. For each vector $X(t)$ in the prediction set, $\{X_{pred}\}$, the $E+1$ neighbors (closest points by Euclidian distance) from the library set $\{X_{lib}\}$ are identified. However, instead of predicting future values of $X(t)$ for points in the prediction set, the prediction is of the corresponding value of $Y(t)$.

The idea has similar aims to Granger's celebrated idea of causality applied widely in economics for linear stochastic systems. However, CCM is formulated for dynamic systems where causes can be interdependent rather than neatly separable. In nonlinear systems, correlations between variables may not be detectable even if they are dynamically coupled. Alternatively, variables can appear correlated for years, but this correlation may disappear even though the dynamics have not changed in a significant way. Such transient correlation followed by apparent lack of stationarity (aka 'mirage correlation', Sugihara et al. 2012), is part of the phenomenology of nonlinear systems that produces the appearance of non-stationarity. Thus, just as 'correlation does not imply causation', in a nonlinear system lack of correlation does not imply lack of causation. Therefore, for systems consisting of nonlinear webs of interacting parts, correlation, though ingrained in our thinking, is fundamentally the wrong tool for identifying relevant variables. Variables (e.g., species) may be dynamically coupled (and be cross-predictable), but show no correlation in time. Cross-predictability means an explanatory variable (or collection of explanatory variables) can be used out-of-sample to predict other coupled, dynamically dependent variables.

Appendix 2: Datasets (appended as Excel files, cvs format) and metadata

Secchi depths (UC Davis): LTP – 1967 to 2020 (every ca.13 days)

Secchi depth measurement - meter
A 25 cm (10 inch) matte white disk is lowered from shaded side of the boat. The depth where disk disappear when lowering and re-appears when raising are recorded and averaged. A subjective measure of viewing conditions and observations of weather and lake conditions are recorded.

Chlorophyll a (UC Davis): LTP – 1983 to 2020; 0, 2, 5, 10, 15, 20, 30, 40, 50, 60, 75, 90, 105 m (depth averaged for upper 30 m and lower depths)

Chlorophyll a measurement - µg/L
Water samples are collected with a Van-Dorn sampler, transferred to 250 mL Nalgene HDPE bottles and stored on ice in an insulated container. 100 mL is filtered through Whatman GF/C glass fiber filters (25mm) within 1-3 hours of sample collection. Filters are kept frozen until analysis. Pigments were extracted by methanol and chlorophyll concentration determined using a Turner Designs 10-AU fluorometer. The final concentration of chlorophyll *a* is determined by correcting for phaephytin by adding a small amount of hydrochloric acid (0.05 mL of 0.3 N HCl to 5 mL of extractant) to the sample and fluorescence remeasured after acidification. The method detection limit is 0.05 µg/L +/- 1.4%. The fluorometer is calibrated annually with the use of *Anacystis nidulans* chlorophyll *a*.

Nitrate (UC Davis): LTP – 1968 to 2020 (every ca.13 days until 2007, and then monthly; 0, 2, 5, 10,15, 20, 30, 40, 50 m (depth averaged)

Nitrate measurement - µg $NO_3 + NO_2$ /L
Water samples are collected with a Van-Dorn sampler, transferred to 250 mL Nalgene HDPE bottles and stored on ice in an insulated container. Subsamples are filtered through Whatman GF/C glass fiber filters (25mm) within 1-3 hours of sample collection and stored at 4ºC. Assays are performed within one week of sample collection.
The analysis method utilizes a hydrazine-copper solution that reduces nitrate to nitrite followed by color development using a diazotization-coupling reaction. The method assumes a 1:1 stoichiometric reduction of nitrate to nitrite. The total nitrite present is then measured with a spectrophotometer at 543 nm. The method's detection limit is 2.0 µg/L; the precision is $\pm$ 0.3 µg/L. Though nitrite is negligible, concentrations are expressed µg $NO_3 + NO_2$ /L.

Kamphake, L.J., S.A. Hannah, and J.M. Cohen. 1967. Automated analysis for nitrate by hydrazine reduction. Water Research. 1:205-216.

Strickland, J.D.H. and T.R. Parsons. 1972. A practical handbook of seawater analysis. Bulletin 167. Fisheries Research Board of Canada, Ottawa, Ontario, Canada.

Lake temperatures (UC Davis): LTP -1967 to 2020 every ca. 13 days)

Temperature measurements – ºC

Temperature profiles from 1967 to 1996 were obtained using several instruments (bathythermograph, hand-held thermometer placed in bucket of water, Martek TMS submersible electronic thermometer, reversing thermometer (protected & unprotected), YSI meter and thermistors.
Temperature profiles were collected between 1996 and 2006 using RBR TDR-200 Brancker TD-200 temperature profiler/depth logger.
Temperature profiles were collected after 2005 using Seabird profilers (SBE19, SBE25, SBE25+). The instruments were factory calibrated.

Stream discharge (ft^3/s) with USGS codes (https://nwis.waterdata.usgs.gov/nwis/uv/):

Upper Truckee River at South Lake Tahoe, CA - UT1 10336610 from 1980
Blackwood Creek near Tahoe City, CA - BC1 10336660 from 1974
Ward Creek at Hwy 89 near Tahoe Pines, CA - WC8 10336676 from 1972

Turnipseed, D. P. and V. B. Sauer, 2010. Discharge Measurements at Gaging Stations. In: U.S. Geological Survey Techniques and Methods book 3, chap. A8. Reston, VA, p. 87

Precipitation and air temperature (National Weather Service via Truckee River Operating Agreement; https://www.troa.net/tis/):
Daily precipitation (inches) and average of maximum and minimum temperatures (ºF) at Tahoe City from 1937

TROA – site 150017 (Lake Tahoe) variables 1616 and 8.
https://www.troa.net/tis/?interval=day&type=1&cat=1&sid=150017&did11=1616&did13=8&format=tab&sdate=01-JAN-1960&edate=01-Apr-2022

Climate Indices: (https://psl.noaa.gov/data/climateindices/)

El Nino index and SOI